Tunable broadband isolator based on electro-optically induced linear gratings in a nonlinear photonic crystal

Zi-yan Yu,[1] Fei Xu,[1,*] Xiao-wen Lin,[1] Xiao-shi Song,[1] Xiao-shi Qian,[1] Qin Wang,[1] and Yan-qing Lu[1,2]

[1]*College of Engineering and Applied Sciences and National Laboratory of Solid State Microstructures, Nanjing University, Nanjing 210093, China*

[2]*e-mail: yqlu@nju.edu.cn*

**Corresponding author: feixu@nju.edu.cn*

Received July 12, 2010; accepted August 28, 2010;
posted September 9, 2010 (Doc. ID 131424); published October 7, 2010

We theoretically propose a broadband optical isolator based on second-harmonic generation in a one-dimensional quadratic nonlinear photonic crystal (NPC) with an embedded defect. An external electric field along the z axis is applied to modulate the NPC refractive index periodically. Complete optical isolation always could be reached with the help of an external field. Influences of the defect position and thickness are discussed. The spectral and power tolerances of the isolator also have been investigated and show high contrast within a wide wavelength range at different power levels. © 2010 Optical Society of America

OCIS codes: 190.0190, 160.2100.

Nonlinear photonic crystals (NPCs) are periodic structures whose optical response depends on the intensity of the light propagating in the crystal [1]. The most common NPC is the quasi-phase-matched (QPM) quadratic nonlinear photonic crystal (QNPC) with a nonlinear grating, whose second-order susceptibility $\chi^{(2)}$ varies periodically [2]. The QNPC has been extensively applied in high-speed signal processing devices, including switches, transistors, modulators, pulse shapers, and isolators [3–5]. As demand keeps increasing for nonmagnetic isolators in integrated photonic systems, more and more attention has been paid to nonreciprocal photonic structures. A lot of promising schemes have been proposed. One of these is the combining of geometrical asymmetry and nonlinear response to realize direction-dependent behavior in the QNPC [6–8]. Perturbed by a suitably designed localized defect, the QPM second-harmonic generation (SHG) in a periodically poled $LiNbO_3$ (PPLN) exhibits a nice optical isolation. The isolation contrast reaches ~1, which is defined as $C = (T^+ + T^-)/(T^+ - T^-)$, where T^+ and T^- are the transmittances along the forward and backward directions, respectively. However, high isolation occurs only in a certain power range and a sharp wavelength range with strict defect parameters [7,8]. To improve the power and spectral tolerance, external tuning is effective. In a PPLN, if an external electric field is applied along the z direction, different domains experience opposite index changes so that a weak linear refractive index grating (LRIG) is induced [9,10]. It further affects the local phase-mismatch condition of each domain during an optical parametric process, while the average phase-mismatch keeps constant. As a consequence, it is possible to improve the performance of a PPLN-based optical isolator through electro-optic (EO) tuning.

In this Letter, we propose an approach to realize a broadband and high-contrast optical isolator by EO tuning of the LRIG in a PPLN. Tolerance of wavelength, input power, defect position, and thickness is studied. By tuning the LRIG, an isolation contrast of nearly 1 can be obtained in a wide range of wavelength, power, defect position, and defect thickness. Considering the benefits of its high-speed and flexible operation, the optical isolator based on a QPM grating with an EO-induced LRIG is promising for future photonic integrated circuits.

As a typical QNPC, PPLN generally includes a grating of a periodic second-order nonlinear coefficient, while the refractive indices of the involved lights are homogeneous, as shown in Fig. 1(a). Here we assume the largest nonlinear coefficient d_{33} is used. n_{1z} and n_{2z} represent the refractive indices of the fundamental wave (FW) and second harmonic (SH), respectively. In this case, the SHG has a wave vector mismatch of $\Delta k = k_{2z} - 2k_{1z}$, resulting from the crystal dispersion. When we apply an electric field along the z axis (optical axis) of the PPLN with intensity E_z, the crystal refractive index ellipsoid deforms accordingly. The refractive indices thus are modulated periodically, because the EO coefficients have

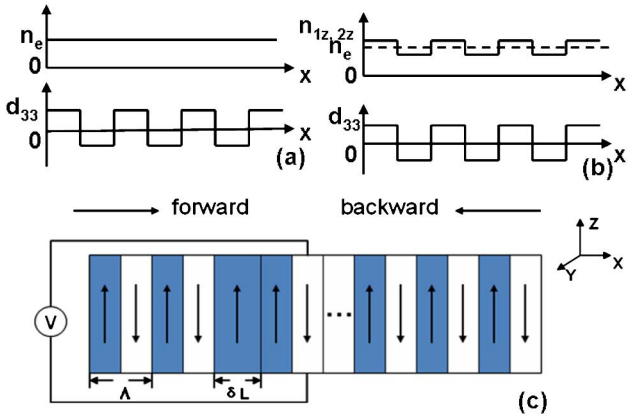

Fig. 1. (Color online) Refractive indices and the second-order nonlinear coefficients in a PPLN: (a) in the absence of an applied electric field and (b) with an electric field applied along the z axis. (c) Schematic diagram of a PPLN isolator with an electric field applied along the z axis. A defect of thickness δL is embedded at the position $x = L_1$, while $L_1 < L/2$.

opposite signs in different domains. In such a situation, both n_{jz} and d_{33} are space dependent. In other words, there are two kinds of gratings built in the crystal simultaneously: a quadratic nonlinear grating (QNLG) and a LRIG, as shown in Fig. 1(b). Therefore, the modified coupling equations are

$$\begin{cases} dE_{1z}/dx = -id_{33}(x)w_1/[n_{1z}(x)c]E_{1z}^{*}E_{2z}e^{-i\Delta k(x)x} \\ dE_{2z}/dx = -id_{33}(x)w_2/[2n_{2z}(x)c]E_{1z}^{2}e^{i\Delta k(x)x} \end{cases},$$
$$n_{jz}(x) = n_{jz} - f(x)n_{jz}^{3}\gamma_{33}E_z/2,$$
$$\Delta k(x) = k_{2z}(x) - 2k_{1z}(x), \qquad k_{jz}(x) = w_j n_{jz}(x)/c, \tag{1}$$

where E_{jz}, ω_j, k_{jz}, and n_{jz} (the subscripts $j = 1, 2$ refer to FW and SH, respectively, and z represents the polarization direction) are the electric fields, the angular frequencies, the wave vectors, and the refractive indices, respectively, and c is the speed of light in a vacuum. γ_{33} is the linear EO coefficient of $LiNbO_3$. $\Delta k = k_{2z} - 2k_{1z}$ is the wave vector mismatch for SHG. The structure function $f(x)$ is $+1$ or -1 in different domains.

Equation (1) was simplified by considering only the first-order Fourier component in a lot of previous theoretical work. However, in our simulation, Eq. (1) is solved numerically by translating it into differential equations without any approximation so that better precision is expected.

To realize an optical isolator function, a localized defect is induced in a PPLN with a duty cycle of 0.5 and a period of $\Lambda = 2l$, as shown in Fig. 1(c), where l is the domain thickness. Here, Λ is set at 18.98 μm to satisfy the QPM condition of $\Delta k = 2\pi/\Lambda$ at 1.55 μm. The crystal length is defined as L. The defect is located at a distance L_1 from $x = 0$ with a thickness $\delta L \neq 0$. After the FW enters the structure from $x = 0$, the cascading process is divided into two parts: the L_1 section and the L–L_1–δL section. The first is a standard SHG without an input SH; the second is a seeded SHG, where both the FW and SH have nonzero initial amplitudes. In this seeded SHG, the initial phases of FW and SH are affected by the defect, whereas the amplitudes are almost unchanged as the propagation distance δL is very short. A similar process will occur when the FW enters the structure from the opposite side ($x = L$). When the defect location and thickness are set properly, the FW intensity at the output end would reach 100% via cascaded up-and-down conversions.

Figure 2 shows the simulation results of the isolation contrast C versus $\delta L/l$ with the defect at the positions $L_1 = 0.2$, 0.25, 0.3, and $0.4L$ for $L = 3.8$ cm. The input FW intensity I is set at 10 MW/cm^2. In the case without the LRIG, the contrast could be close to 1 by selecting a suitable defect location and thickness. When the asymmetry is strong ($L_1 = 0.2$ or $0.25L$), it is easy to achieve a high contrast (>0.95) in a wide range of δL. However, when the asymmetry is weak ($L_1 = 0.3$ or $0.4L$), it is difficult to achieve high contrast. The contrast almost drops to zero at $\delta L/l > 0.5$. However, in the case with the EO-induced LRIG, the device shows great isolation (nearly 1) in a wide range of δL and L_1 with an optimized voltage applied.

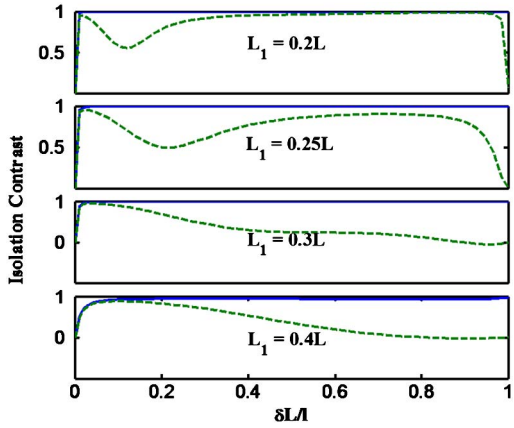

Fig. 2. (Color online) Isolation contrast C of the FW versus $\delta L/l$ when the defect is placed at positions $L_1 = 0.2$, 0.25, 0.3, and $0.4L$ for $L = 3.8$ cm and $I = 10$ MW/cm^2. The blue solid and green dashed curves refer to the condition with and without the LRIG, respectively.

In fact, all the optical isolators based on the nonlinear effect suffer from the problem of pumping intensity tolerance, including the isolator based on PPLN. As shown in Fig. 3(a), the contrast depends seriously on the FW intensity for $L_1 = 0.25L$ and $\delta L/l = 0.5$. The blue solid and green dashed curves refer to the condition with and without the LRIG, respectively. In the case without the LRIG, a maximum isolation contrast of around 0.9 is reached at the input FW intensity of 9 MW/cm^2. When the input FW intensity is weak, the isolation contrast keeps increasing from zero. As the input FW intensity goes higher, it drops quickly. However, the situation is greatly improved with an EO-induced LRIG. The isolation contrast stays over 96% when $I > 5$ MW/cm^2. Figure 3(b) shows the contrast depending on both a different FW intensity and defect length by tuning the LRIG, with $L_1 = 0.25L$. Perfect isolation can be obtained when $I > 5$ MW/cm^2 and $\delta L > 0.2l$. The higher tolerance in FW intensity, defect length, and position is attributed to the asymmetry of the QNLG and the EO-induced LRIG.

Bandwidth is also one of the key factors of nonlinear-effect-based isolators. Everything discussed above is under the perfect QPM condition, $\Delta k'L = \Delta kL - 2\pi/\Lambda$, defined as the bandwidth. It equals zero at the central

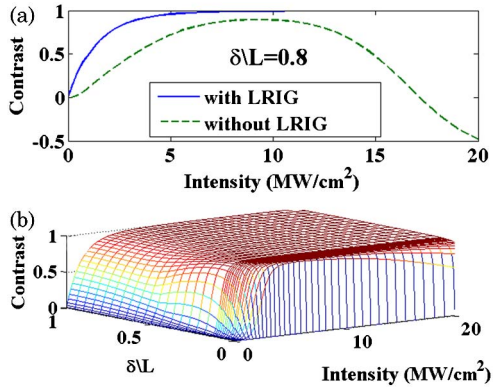

Fig. 3. (Color online) Isolation contrast C of the FW versus the (a) input FW intensity for $L_1 = 0.25L$ and $\delta L/l = 0.5$ and (b) input FW intensity and defect length by electro-optically tuning the LRIG. The blue solid and green dashed curves refer to the condition with and without the LRIG, respectively.

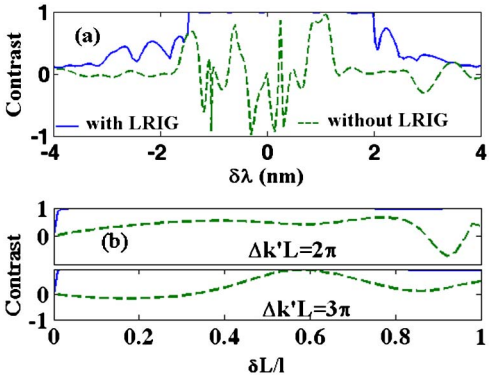

Fig. 4. (Color online) Isolation contrast C: (a) at a wide range near the central wavelength and (b) versus the defect thickness when the QPM condition is not satisfied ($\Delta k'L = 2\pi$ or 3π). $I = 10$ MW/cm^2, $\delta L/l = 0.5$, and $L_1 = 0.25L$. The blue solid and green dashed curves refer to the condition with and without the LRIG, respectively.

wavelength where the QPM condition is satisfied. When the FW deviates from the central wavelength in a wide range, the contrast oscillates close to zero if there is no EO-induced LRIG, as shown in Fig. 4(a). The poor bandwidth comes from the strict limitation of the QPM condition and a uniform grating. With an EO-induced LRIG, the Fourier vector of QNLG can be shifted and phase mismatch can be compensated as much as possible. High contrast with a wide bandwidth can be achieved. Here $I = 10$ MW/cm^2, $\delta L/l = 0.5$, and $L_1 = 0.25L$. The blue solid and green dashed curves refer to the condition with and without the LRIG, respectively. We have also investigated isolation versus the defect thickness when the QPM condition is not satisfied ($\Delta k'L = 2\pi$ or 3π), as shown Fig. 4(b). The contrast is still poor without the EO-induced LRIG. However, with the EO-induced LRIG, the isolation contrast of $\sim$1 can be achieved in a wide range of $\delta L/l$. High contrast and large tolerance at $\delta L/l = 0.5$, which is assumed in the above simulation model, are proven. In Fig. 4, the isolation contrast is asymmetric near the central wavelength without the LRIG because of the material dispersion and the asymmetric mismatch $\Delta k'L$.

There are also other external tuning methods that may control the QPM parametric process in an asymmetric PPLN, for example, temperature or the acousto-optic effect. These methods are similar in purpose, but their mechanisms and performances are different. Temperature tuning can slightly shift the QPM wavelength and expand the working bandwidth, but it cannot help enlarge the power tolerance. An acousto-optic-effect-induced grating can rotate the polarization direction of the FW or SH and hence affect the energy transmission between the FW and SH. The tolerances of both defect length and position are enhanced, while the bandwidth is limited because two strict phase matching conditions are not easy to satisfy simultaneously. An EO-induced LRIG can increase the tolerance of the input FW intensity, defect length, defect position, and wavelength bandwidth. It is also easier to realize in photonic integrated circuits owing to the fast response and flexible manipulation. In our simulation, the tuning range of the applied electrical fields is 0–1 kV/mm: it is possible to improve the isolation a little by applying a larger electrical field, but too high a voltage is not preferred for practical applications.

In summary, we proposed an EO-tunable broadband optical isolator based on SHG in a one-dimensional QNPC with an embedded defect. The external electric field greatly improves the isolating performance. A broadband isolator with high contrast and large wavelength tolerance is successfully demonstrated in theory.

We acknowledge financial support from the National 973/Quantum Manipulation Program under contracts 2010CB327803 and 2006CB921800 and the National Natural Science Foundation of China (NSFC) under contracts 60977039 and 10874080. Zi-yan Yu acknowledges support from the Scientific Research Foundation of the Graduate School of Nanjing University under contract 2009CL01.

References

1. V. Berger, Phys. Rev. Lett. **81**, 4136 (1998).
2. S. Saltiel and Y. S. Kivshar, Opt. Lett. **25**, 1204 (2000).
3. M. F. Yanik, S. Fan, and M. Soljačić, Appl. Phys. Lett. **83**, 2739 (2003).
4. M. F. Yanik, S. H. Fan, M. Soljačić, and J. D. Joannopoulos, Opt. Lett. **28**, 2506 (2003).
5. H. Nakamura, Y. Sugimoto, K. Kanamoto, N. Ikeda, Y. Tanaka, Y. Nakamura, S. Ohkouchi, Y. Watanabe, K. Inoue, H. Ishikawa, and K. Asakawa, Opt. Express **12**, 6606 (2004).
6. Z. F. Yu and S. H. Fan, Nat. Photon. **3**, 91 (2009).
7. K. Gallo and G. Assanto, J. Opt. Soc. Am. B **16**, 267 (1999).
8. K. Gallo, G. Assanto, K. R. Parameswaran, and M. M. Fejer, Appl. Phys. Lett. **79**, 314 (2001).
9. F. Xu, J. Liao, X. J. Zhang, J. L. He, H. T. Wang, and N. B. Ming, Phys. Rev. A **68**, 033808 (2003).
10. F. Xu, J. L. He, J. Liao, Q. Wang, Q. Xu, N. H. Shen, H. T. Wang, and N. B. Ming, Phys. Rev. A **68**, 053803 (2003).